A Comprehensive Scheduling Framework using SP-ADMM for Residential Demand Response with Weather and Consumer Uncertainties

Xiao Kou, *Student Member, IEEE*, Fangxing Li, *Fellow, IEEE,* Jin Dong, *Member, IEEE,* Mohammed Olama, *Senior Member, IEEE,* Michael Starke, *Member, IEEE,* Yang Chen, *Member*, *IEEE*, Helia Zandi, *Member, IEEE*

***Abstract*— This paper presents a comprehensive scheduling framework for residential demand response (DR) programs considering both the day-ahead and real-time electricity markets. In the first stage, residential customers determine the operating status of their responsive devices such as heating, ventilation, and air conditioning (HVAC) systems and electric water heaters (EWHs), while the distribution system operator (DSO) computes the amount of electricity to be purchased in the day-ahead electricity market. In the second stage, the DSO purchases insufficient (or sells surplus) electricity in the real-time electricity market to maintain the supply-demand balance. Due to its computational complexity and data privacy issues, the proposed model cannot be directly solved in a centralized manner, especially with a large number of uncertain scenarios. Therefore, this paper proposes a combination of stochastic programming (SP) and the alternating direction method of multipliers (ADMM) algorithm, called SP-ADMM, to decompose the original model and then solve each sub-problem in a distributed manner while considering multiple uncertain scenarios. The simulation study is performed on the IEEE 33-bus system including 121 residential houses. The results demonstrate the effectiveness of the proposed approach for large-scale residential DR applications under weather and consumer uncertainties.**

***Index Terms*—Demand response (DR), home energy management system (HEMS), electric water heater (EWH), HVAC, distribution system operator (DSO), stochastic programming based alternating direction method of multipliers (SP-ADMM), uncertainty.**

Abbreviations

EWH	Electric water heater.
HEMS	Home energy management system.
HVAC	Heating, ventilation, and air conditioning.

Sets and Indices

d	Index of iterations.
N_M / j, k	Set/index of buses (aggregators).
C_k	Set of child buses of bus k.
N_N / i	Set/index of residential customers.
Ns / s	Set/index of scenarios.
N_T / t	Set/index of time.

Constants

a / b	Electricity cost coefficients.
c^{water}	Specific heat capacity of water (J/(kg·℃)).
C_i^{house}	Thermal capacitance of house i (J/℃).
C_i^{wh}	Thermal capacitance of the EWH in house i (J/℃).
$m_{i,t,s}^{water}$	Hot water consumption of house i at time t in scenario s (kg).
p_i^{hvac} / q_i^{hvac}	Real/reactive power rating of the HVAC in house i (kW).
$p_{i,t,s}^{nr}$ / $q_{i,t,s}^{nr}$	Real load of the non-responsive devices in house i at time t in scenario s (kW).
$\overline{P}^{pcc}$	Maximum contracted load limit at the PCC (kW).
$p_{i,t,s}^{pv}$	PV generation of house i at time t in scenario s (kW).
p_i^{wh} / q_i^{wh}	Real/reactive power rating of the EWH in house i (kW).
r_{j-k}^{line} / x_{j-k}^{line}	Resistance/reactance of the distribution line connecting bus j and bus k (Ω).
R_i^{house}	Thermal resistance of house i (℃/kW).
R_i^{wh}	Thermal resistance of the EWH in house i (℃/kW).
$\underline{T}_i^{in}$ / $\overline{T}_i^{in}$	Minimum/maximum indoor temperature limit of house i (℃).
T_i^{ins}	Indoor temperature setpoint of house i (℃).
$T_{i,t,s}^{out}$	Outdoor temperature forecast at time t in scenario s (℃).
$\underline{T}_i^{wh}$ / $\overline{T}_i^{wh}$	Minimum/maximum water temperature limit of the EWH in house i (℃).
T_i^{whs}	Hot water temperature setpoint of house i (℃).
V^{pcc}	Voltage magnitude at the PCC.
α / β	Weight factors ($/℃).
ε^R / ε^S	Primary/secondary tolerance value.
Δt	Length of the time interval.
λ^{rtp} / λ^{rts}	Electricity purchasing/selling price in the real-time market ($/kW).
λ^{vio}	Peak load violation rate ($/kW).
ρ	Penalty factor of the augmented Lagrangian term.

Continuous Variables

$dis_{i,t,s}^{hvac}$	Indoor temperature discomfort of customer i at time t in scenario s (℃).
$dis_{i,t,s}^{wh}$	Water temperature discomfort of customer i at time t in scenario s (℃).
$I_{j-k,t,s}^{line}$	Power flow of line j-k at time t in scenario s.
$p_{i,t,s}^{cus}$ / $q_{i,t,s}^{cus}$	Real/reactive load of house i at time t in scenario s (kW / kVar).
$p_{j,t,s}^{agg}$ / $q_{j,t,s}^{agg}$	Real/reactive load of aggregator j at time t in scenario s (kW/kVar).
$p_{j-k,t,s}^{line}$ / $q_{j-k,t,s}^{line}$	Real/reactive power flowing from node j to node k at time t in scenario s (kW/kVar).

$p_{t,s}^{da}$ The amount of electricity purchased from the day-ahead market at time t in scenario s (kW).

$p_{t,s}^{pcc}$ Actual load at the PCC at time t in scenario s (kW).

$p_{t,s}^{rtp}$ / $p_{t,s}^{rts}$ The amount of electricity purchased from/sold to the real-time market at time t in scenario s (kW).

p_{s}^{vio} The maximum amount of load that exceeds the contracted load limit in scenario s (kW).

$R_{t,s}$ Primal residual of ADMM at time t in scenario s.

$S_{i,t,s}$ Secondary residual of house i at time t in scenario s.

$T_{i,t,s}^{in}$ Indoor temperature of house i at time t in scenario s (℃).

$T_{i,t,s}^{wh}$ Water temperature of the EWH in house i at time t in scenario s (℃).

$V_{j,t,s}$ Voltage magnitude of bus j at time t in scenario s.

$\lambda_{t,s}$ Dual variable associated with the power balance equation at time t in scenario s.

Binary Variables

$b_{i,t}^{hvac}$ Operating status of the HVAC in house i at time t.

$b_{i,t}^{wh}$ Operating status of the EWH in house i at time t.

I. Introduction

THE ever-increasing electric load and growing renewable integration pose severe threats to the secure and economic operations of power grids [1]. One solution to address this challenge is implementing the demand response (DR) [2]. Existing DR programs are primarily designed for industrial and commercial customers, who tend to have larger electric loads that are more easily targetable [3]. However, residential loads account for 38% of the total energy consumption in the United States, indicating the significant potential in this sector [4]. Since residential loads are composed of numerous low-capacity home appliances, it is imperative to have an effective algorithm that can coordinate the operating schedules of residential components and devices at scale to improve the DR impact and performance [5].

In recent years, advances in communication technologies have provided tremendous opportunities for grid operators to send messages to (or receive messages from) residential customers through secured two-way communication channels [6]. With the support of home energy management systems (HEMSs), distribution system operators (DSOs) can connect with customers to realize system-wide control objectives, e.g., DR. Existing control structures for residential DR programs are categorized into centralized and distributed [7]. In [8]-[9], residential DR management problems are formulated as centralized models, where the control actions are computed and executed by the control center according to the measurements from sub-systems. Centralized approaches are straightforward and applicable to small-scale networks with customers sharing common goals. However, in a centralized approach, end-users may have to release their device operation information and allow the utility to control their appliances. Moreover, as the number of customers grows, the computational complexity will increase significantly. In [10]-[11], distributed residential DR models are proposed, where customers independently conduct local optimizations to determine the optimal scheduling of devices. The major part of the calculation is performed by local HEMSs, distributing intelligence and reducing the centralized computational requirements. Since each HEMS is independent, calculations are all run in parallel, reducing the needed computational time. Meanwhile, privacy can also be better protected, as only minimal information is shared with the electric utility company.

In addition to the scalability and privacy issues, residential DR programs may also confront the challenges of handling uncertain parameters, e.g., weather and consumer uncertainties. The conventional approaches treat the uncertain parameters as fixed values. However, as the forecasting technology is still immature, extra spinning reserve capacity and supplemental reserve have to be ensured, which increases the electricity cost. To address this challenge, attention has been paid to optimization methods that model uncertainty and fluctuation as non-constant values [12]. In [13], a robust optimization model is proposed to shave the system peak load and save residential customers' electricity bills while considering weather and occupancy uncertainties. The results indicate that the aggregator can still reduce the peak load even in the worst case where none of the customers agree with the system-level objectives. Generally, the inputs for robust optimization are the bounds of the uncertain parameters. This allows robust optimization to avoid the risks of constraint violations in extreme conditions. In [14], a stochastic programming (SP) model for HEMSs is presented, which aims to save customers' electricity costs while considering the uncertainties of both the availability of electric vehicles (EVs) and renewable generation. The results demonstrate that residential customers can save up to 31% of their electricity costs as compared to the deterministic approach. Unlike robust optimization, SP assumes that the uncertain parameters comply with certain probabilistic distributions, such that it can be converted to an equivalent deterministic problem. In [15], SP and robust optimization are applied to solve a real-time price-based DR management problem. The results suggest that both approaches can mitigate the financial risk introduced by price uncertainty.

The literature includes additional works that also target residential DR solutions using home appliances. In [16], an asynchronous bottom-up scheme is presented to coordinate the operations of distributed energy resources, including EVs, thermostat-controlled loads, and energy storage systems. This approach couples a device's dynamic state to a stochastic request rate for electricity services, and it perturbs the responsive devices' ON/OFF transition rates to create flexibility for the virtual power plant operator. In [17]-[18], a linear time-invariant thermal energy storage model, which is equivalent to a virtual battery state-of-charge model, is proposed to capture the dynamics of aggregated thermostat-controlled loads. This approach significantly reduces the computational burden, and it allows constraints that couple system-level and house-level variables. However, a lookup table that relates the thermal energy storage model to measurement conditions has to be developed. Moreover, if a

new condition is encountered in the future, the parameters of the thermal energy storage model must be re-identified. In [19], a bi-level optimization model is used to flatten the system-level load curve and minimize the cost of residential customers. The problem is converted to an equivalent single-level problem and then solved with an iterative distributed algorithm. However, this approach does not consider the network losses and the temperature dynamics for thermostat-controlled loads (e.g., heating, ventilation, and air conditioning (HVAC) systems and electric water heaters (EWHs)). In [20], the mathematical models of major home appliances (e.g., fridge, freezer, dishwasher) are formulated. A mixed-integer linear programming model is developed to minimize the energy consumption, energy cost, emissions, and peak load of the residential energy hubs in smart grids. The deficiencies of this work are that the proposed approach is not scalable, and the impact of uncertain parameters (e.g., weather and consumer behaviors) on system performance is not considered. In [21], a two-stage optimization model is presented to optimize the customers' energy consumption patterns and improve grid operational efficiency. Again, the uncertainties introduced by renewable and customer activities are ignored. In [22], a scalable and distributed algorithm is developed for managing the operating schedules of home appliances. However, the weather and customers' uncertainties are not considered.

In summary, even though existing research has already explored residential DR problems, there is still a lack of a comprehensive scheduling framework considering the weather and consumer uncertainties while coordinating the operating schedules of numerous home devices at scale. To bridge this gap, a two-stage SP model is formulated to maximize community social welfare. Then it is decomposed into DSO-level and house-level sub-problems with the alternating direction method of multipliers (ADMM) algorithm. The proposed approach is thus called the SP-ADMM approach. Instead of formulating an aggregated thermal energy storage model as suggested in [17]-[18], the proposed approach handles the scalability problem from another perspective by decomposing the original model into sub-problems and solving it in a distributed manner. By doing so, the requirement for building the lookup table is eliminated. Further, if compared with [20]-[22], the proposed model takes the weather and consumers' uncertain behaviors into consideration. The performance improvement is verified by the case study in the later sections of this paper. To conclude, the main contributions of this paper are as follows:

1) A comprehensive scheduling framework that considers both the day-ahead and real-time electricity markets is proposed to mitigate the impacts of weather and consumers' behavior uncertainties on residential DR performance;

2) A limited information exchange mechanism is developed among the DSO, load aggregators (LAs), and end-consumers to better protect residential customers' privacy;

3) A new algorithm called the SP-ADMM is proposed, which combines SP and the ADMM algorithm. The proposed approach decomposes the original model into sub-problems to ensure its feasibility for large-scale applications while considering a large number of uncertain scenarios; and

4) A comparison study is conducted to evaluate the performance of the conventional approach, the deterministic approach, and the proposed SP-ADMM approach. The outcome can serve as benchmarking results for future works in residential DR.

The rest of this paper is structured as follows: Section II presents the architecture of the residential distribution networks, Section III formulates the proposed comprehensive framework for residential DR, Section IV discusses the solution algorithm, Section V conducts the case studies, and Section VI concludes the paper.

Notation conventions: superscript ^{hvac} refers to HVAC, superscript ^{wh} refers to EWH, superscript ^{cus} refers to residential customers, superscript ^{agg} refers to LAs, and superscript ^{line} refers to distribution lines.

II. Residential Distribution Network Architecture

The proposed residential distribution network has a hierarchical architecture, including the DSO, LAs, and residential customers, which are the top, middle, and bottom levels, respectively. The reason for introducing LAs is that the flexible load resource of a single residential customer is far less than the DSO's minimum capacity threshold. LAs can collect the small load resources for the DSO and help residential customers to participate in the electricity market [23]-[24]. Moreover, LAs reduce the DSO communication requirements since communication needs are now decreased to a single entity instead of many assets.

In this work, it is assumed that LAs are profit-neutral entities. The revenue of LAs comes from those customers who participate in the DR program. Each customer is required to pay a fixed amount of membership fee to its corresponding aggregator to access the electricity market. Moreover, any excess payment will be refunded, and deficiency will be repaid at the end of each month, which is similar to the business model of independent system operators (ISO). However, since the operation cost of aggregators is out of the scope of this work, the details can be explored in future works.

Also, residential customers are assumed to be clustered by their geographical locations and interconnected to the distribution system through LAs. In real-world applications, LAs may have customers subscribed from different locations of the distribution network. However, the cost of implementing a DR aggregator is associated with the distances from the central aggregation point to individual flexible resources. So, although each LA may have different customers subscribed, we can always model and cluster DR loads based on locations (nodes). This practice of clustering DR loads based on locations is aligned with [25]-[26]. The authors of [26] solve the distributed flexible resources aggregation problem by minimizing the sum of distances from the central aggregation point to individual flexible resources. Therefore, it is usually more economical for aggregators to cluster residential customers based on their geographical locations. From the power flow viewpoint, LAs are viewed as buses and interconnected to form a distribution network.

At the house level, HEMSs are responsible for receiving data from the LAs and local weather service centers to perform optimization and decision-making on behalf of customers. The responsive devices considered are HVAC systems and EWHs.

III. Mathematical Formulation

Four types of uncertain parameters are studied in this paper, including 1) outdoor temperature, 2) solar generation, 3) non-responsive load, and 4) hot water consumption. To reduce the impact of uncertain parameters, a two-stage scheduling model has been formulated. In the first stage, residential customers determine the operating status of responsive devices, while the DSO computes the amount of electricity needed to be purchased in the day-ahead market. In the second stage, the DSO purchases insufficient (or sells surplus) electricity in the real-time market to maintain the supply-demand balance. A graph illustrating this process is provided in Fig. 1.

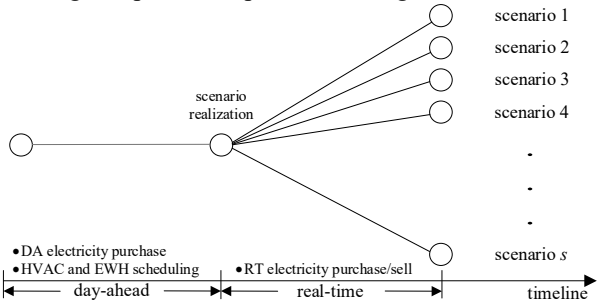

Fig. 1. The proposed two-stage residential management process.

A. Objective function

The objective of the residential DR program is to maximize the community social welfare, as described by:

$$\min f(x) + E\left[Q(x,\xi)\right] \tag{1}$$

$$f(x) = \sum_{t\in N_T}\left[a\cdot\left(p_t^{da}\right)^2 + b\cdot p_t^{da}\right] \tag{2}$$

$$\begin{aligned} Q(x,\xi) = {} & \lambda^{vio}\cdot p_s^{vio} + \sum_{t\in N_T}\left(\lambda^{rtp}\cdot p_{t,s}^{rtp} - \lambda^{rts}\cdot p_{t,s}^{rts}\right) \\ & + \sum_{t\in N_T}\sum_{i\in N_N}\left(\alpha\cdot dis_{i,t,s}^{hvac} + \beta\cdot dis_{i,t,s}^{wh}\right) \end{aligned} \tag{3}$$

where $f(x)$ represents the first-stage objective, $Q(x, \xi)$ represents the second-stage objective, (2) calculates the DSO's electricity purchasing cost in the day-ahead market represented by a quadratic function [27], (3) calculates the sum of peak load violation charge, electricity trading cost in the real-time market, and customers' discomfort cost.

Note that in (3), the peak load violation charge is defined as the product of a peak load violation rate and the maximum amount of load that exceeds the contracted load limit at the point of common coupling (PCC) [28]. The load violation amount can be calculated from (4) and (5).

$$p_{t,s}^{pcc} = p_t^{da} + p_{t,s}^{rtp} - p_{t,s}^{rts} \tag{4}$$

$$p_s^{vio} = \max\left(p_{t,s}^{pcc} - \overline{p}^{pcc}, 0\right) \tag{5}$$

In practical application, the discomfort weight factors may vary from case to case, and they should be determined by the DR participants. If customers prefer comfort over saving money, then larger values should be assigned, whereas if customers prefer to save more money, then smaller values should be chosen. In other words, this paper is a methodology paper, and we provide a technical approach to scheduling DR while the decision makers (i.e., DR participants) may select weight factors based on their own preferences.

B. HVAC model

The input parameter for the HVAC model is the forecasted outdoor temperature in each scenario. The details of the HVAC model are available in the Appendix. The discrete-time form of the HVAC model is represented by:

$$T_{i,t,s}^{in} = T_{i,t-1,s}^{in} + \left[\left(T_{i,t,s}^{out} - T_{i,t-1,s}^{in}\right)/R_i^{house} - b_{i,t}^{hvac}\cdot P_i^{hvac}\right]\cdot\Delta t / C_i^{house} \tag{6}$$

$$\underline{T}_i^{in} \le T_{i,t,s}^{in} \le \overline{T}_i^{in} \tag{7}$$

$$dis_{i,t,s}^{hvac} = \left|T_{i,t,s}^{in} - T_i^{ins}\right| \tag{8}$$

where (6) calculates the indoor temperature of house i at each time in different scenarios, (7) is the minimum/maximum indoor temperature limit constraint for each house, and (8) calculates customers' discomfort due to indoor temperature deviating from the setpoint in different scenarios.

C. EWH model

The input parameter for the EWH model is the indoor temperature and the amount of hot water consumption in each scenario. The discrete-time form of the EWH model is represented by:

$$\begin{aligned} T_{i,t,s}^{wh} = {} & T_{i,t-1,s}^{wh} + \left[\left(T_{i,t,s}^{in} - T_{i,t-1,s}^{wh}\right)/R_i^{wh}\right. \\ & \left. - c^{water}\cdot m_{i,t,s}^{water}\left(T_{i,t-1,s}^{wh} - T_{i,t,s}^{in}\right) + b_{i,t}^{wh}\cdot P_i^{wh}\right]\cdot\Delta t / C_i^{wh} \end{aligned} \tag{9}$$

$$\underline{T}_i^{wh} \le T_{i,t,s}^{wh} \le \overline{T}_i^{wh} \tag{10}$$

$$dis_{i,t,s}^{wh} = \left|T_{i,t,s}^{wh} - T_i^{whs}\right| \tag{11}$$

where (9) calculates the water temperature of house i at each time in different scenarios, (10) is the minimum/maximum water temperature limit constraint for each house, and (11) calculates customers' discomfort due to water temperature deviating from the setpoint in different scenarios.

D. Load model

In this work, the power output of the solar photovoltaic (PV) is viewed as a negative load. Therefore, the load of each house is equal to the sum of the responsive load (including HVAC and EWH) and the non-responsive load minus the solar generation. The load model is given by:

$$p_{i,t,s}^{cus} = p_i^{hvac}S_{i,t}^{hvac} + p_i^{wh}S_{i,t}^{wh} + p_{i,t,s}^{nr} - p_{i,t,s}^{pv} \tag{12}$$

$$q_{i,t,s}^{cus} = q_i^{hvac}S_{i,t}^{hvac} + q_i^{wh}S_{i,t}^{wh} + q_{i,t,s}^{nr} \tag{13}$$

where (12) calculates the real power load of each house in different scenarios, and (13) calculates the reactive power load of each house in different scenarios.

E. Network model

The DistFlow equations in [29] are applied to solve the network flow problem in the distribution network. The mathematical formulations for a distribution network flow are given as follows:

$$p_{j,t,s}^{agg} = \sum_{i\in j} p_{i,t,s}^{cus} \tag{14}$$

$$q_{j,t,s}^{agg} = \sum_{i\in j} q_{i,t,s}^{cus} \tag{15}$$

$$p_{j-k,t,s}^{line} = \sum_{\forall k-C_k} p_{k-C_k,t,s}^{line} + r_{j-k}^{line}\cdot\left(I_{j-k,t,s}^{line}\right)^2 + p_{k,t,s}^{agg} \tag{16}$$

$$q_{j-k,t,s}^{line} = \sum_{\forall k-C_k} q_{k-C_k,t,s}^{line} + x_{j-k}^{line}\cdot\left(I_{j-k,t,s}^{line}\right)^2 + q_{k,t,s}^{agg} \tag{17}$$

$$|V_{k,t,s}|^2 = |V_{j,t,s}|^2 - 2\left(r^{line}_{j-k}\cdot p^{line}_{j-k,t,s} + x^{line}_{j-k}\cdot q^{line}_{j-k,t,s}\right) + \left(I^{line}_{j-k,t,s}\right)^2 \cdot \left[\left(r^{line}_{j-k}\right)^2 + \left(x^{line}_{j-k}\right)^2\right] \quad (18)$$

$$\left(p^{line}_{j-k,t,s}\right)^2 + \left(q^{line}_{j-k,t,s}\right)^2 \le \left(V_{j,t,s}\right)^2 \cdot \left(I^{line}_{j-k,t,s}\right)^2 \quad (19)$$

$$p^{pcc}_{t,s} = p^{line}_{0-1,t,s} \quad (20)$$

where (14) calculates the net real load at aggregator j in different scenarios, (15) calculates the reactive load at aggregator j in different scenarios, (16) and (17) respectively represent the net real and reactive branch power flow of line j-k at time t in different scenarios, (18) calculates the voltage magnitude of each bus k at each time in different scenarios, (19)is the branch flow constraint, and (20) is the power balance constraint at the PCC.

Note that if $(V_{j,t,s})^2$, $(V_{j,t,s})^2$ and $(Iline\ j\text{-}k,t,s)^2$ are viewed as variables, constraints (16)-(18) are linear, and (19) becomes a second-order cone constraint after relaxing the "equal" sign to the "less than or equal" sign.

IV. Solution Algorithm

The above model involves a large number of variables if a centralized optimization algorithm is applied. For example, in the next section of case studies, the IEEE 33-bus system including 121 residential houses will be used as the test system, where the optimization problem has 887,040 continuous variables, 23,232 binary variables, 654,720 equality constraints, and 1,059,168 inequality constraints.

Due to the massive problem size, it would be difficult to directly solve this model with available solvers. Therefore, the ADMM is introduced to decompose the original problem into a DSO-level problem and a set of house-level sub-problems to reduce the computational complexity. Meanwhile, there are multiple uncertain scenarios in the residential DR behavior, so a mathematical model considering such uncertainties must be addressed as well. Therefore, we propose a solution algorithm called the SP-ADMM, which combines SP and the ADMM algorithm to solve the proposed model in Section III. The proposed SP-ADMM algorithm for solving comprehensive DR scheduling is illustrated next.

A. Decomposing the centralized model with the ADMM

The ADMM is a robust iteration-based algorithm that solves arbitrary-scale optimization problems and supports distributed computation. More details on the ADMM algorithm are available in [30]. In this work, the DSO and customers have separable objectives. The coupling constraint is the supply-demand balance constraint in (20), which contains variables from both the utility-level and house-level. Therefore, the proposed centralized model can be decomposed into a utility-level optimization problem and a set of house-level optimization problems for efficient computation.

The primary residual and the secondary residual in the ADMM algorithm are calculated by (21) and (22), respectively:

$$R^{(d)}_s = p^{pcc,(d)}_s - p^{line,(d)}_{0-1,s} \quad (21)$$

$$S^{(k)}_{i,s} = \rho\cdot\left(p^{cus,(d)}_{i,s} - p^{cus,(d-1)}_{i,s}\right) \quad (22)$$

The dual variable associated with the coupling constraint is calculated by:

$$\lambda^{(d)}_s = \lambda^{(d-1)}_s + \rho\cdot R^{(d)}_s \quad (23)$$

Note that the iteration number in the ADMM is related to the value of penalty factor ρ. Generally, a smaller ρ yields better optimization results, but it comes with the risk of convergence issues. On the other hand, a larger ρ may give a sub-optimal solution, but it makes the algorithm easier to converge. Therefore, the value of ρ may differ from case to case in practical applications.

1) House-level sub-problem

The customers' objectives are to minimize indoor and hot water discomfort costs. The decision variable includes the operating schedules of HVACs and EWHs for the next day. Therefore, the deterministic equivalent of the house-level optimization problem can be represented by:

$$\begin{aligned}&\min \sum_{t\in N_T}\sum_{s\in N_S}\left(\alpha\cdot dis^{hvac}_{i,t,s} + \beta\cdot dis^{wh}_{i,t,s}\right)\\ &+\sum_{t\in N_T}\sum_{s\in N_S}\rho_s\cdot\left\{\lambda_t\left[R^{(d)}_{t,s}/N_N - p^{cus,(d-1)}_{i,t,s} + p^{cus}_{i,t,s}\right]\right\}\\ &+\sum_{t\in N_T}\sum_{s\in N_S}\rho_s\cdot\left\{\frac{\rho}{2}\cdot\left\|R^{(d)}_{t,s}/N_N - p^{cus,(d-1)}_{i,t,s} + p^{cus}_{i,t,s}\right\|^2_2\right\}\end{aligned} \quad (24)$$

where the first two terms minimize the customers' discomfort cost, and the remaining terms present the penalty for violating the power balance constraints.

The constraints for the house-level optimization problem are (6)-(13), and (22).

2) LA-level calculation

The aggregator-level calculation collects local real and reactive load information and reports it to the DSO, as given by (14)-(15).

3) DSO-level sub-problem

The utility's objectives are to minimize the contracted load violation charge plus the electricity purchasing cost in both the day-ahead and real-time electricity markets. The decision variables are the amount of electricity purchased from and sold to the electricity markets. The deterministic equivalent of the DSO-level objective function becomes:

$$\begin{aligned}&\min \sum_{t\in N_T}\left[a\cdot\left(p^{da}_t\right)^2 + b\cdot p^{da}_t\right] + \sum_{s\in N_S}\rho_s\cdot\lambda^{vio}\cdot p^{vio}_s\\ &+\sum_{t\in N_T}\sum_{s\in N_S}\rho_s\cdot\left(\lambda^{rtp}_s\cdot p^{rtp}_{t,s} - \lambda^{rts}_s\cdot p^{rts}_{t,s}\right) + \sum_{t\in N_T}\sum_{s\in N_S}\rho_s\cdot\left(\lambda_{t,s}\cdot R^{(d)}_{t,s} + \frac{\rho}{2}\cdot\left\|R^{(d)}_{t,s}\right\|^2_2\right)\end{aligned} \quad (25)$$

where the first two terms represent the electricity purchasing cost in the day-ahead market, the third term is the peak load violation charge, the fourth and fifth terms are the cost/revenue for trading electricity in the real-time electricity market, and the rest represents the penalty terms for violating the power balance constraints.

The constraints for the DSO level optimization problem are (4)-(5), (16)-(19), (21), and (23).

B. Information exchange between agents

The messages sent from the DSO through LAs to all the customers are arrays that contain the primary residuals in the ADMM algorithm and the dual variables associated with the power balance equation in each scenario (i.e., *R(d) s* and *λ (d) s*). The messages sent from customers to their corresponding LAs are arrays that contain the total real and reactive load usage data in each scenario (i.e., *pcus i,t,s* and *qcus i,t,s*). Finally, the messages sent from LAs to the DSO are the total real and reactive power consumption within their service region in each

scenario (i.e., *pagg i,t,s* and *qagg i,t,s*). As such, the information exchange between the aggregator/DSO and the load is minimal to best maintain the data security of the consumers.

C. Flowchart of the proposed algorithm

The flowchart of using the ADMM algorithm to solve the two-stage residential DR management problem is given in Fig. 2. During the iteration process, the house-level HEMS receives the arrays of the primal residual in the ADMM and the dual variables associated with the power balance equations in each scenario. Then each HEMS locally updates the real/reactive load consumption data in each scenario accordingly. The aggregator is responsible for calculating the total load within its service region and passing the information to the DSO. Finally, the DSO receives the real/reactive load information from each aggregator and updates the primal residuals and dual variables associated with the coupling constraints in each scenario. The iteration will stop when both $||R(d)\ s||_2$ and $||S(d)\ i||_2$ satisfy the tolerance criteria.

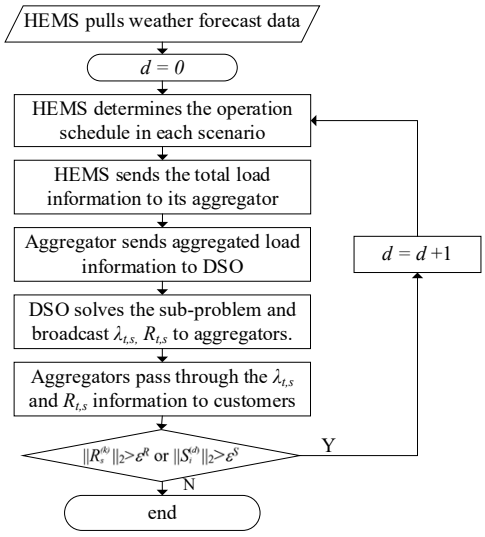

Fig. 2. Flowchart of the proposed algorithm.

V. Case Study

The proposed algorithm is tested on the IEEE 33-bus system including 121 residential houses. As mentioned in Section IV, the optimization model has 887,040 continuous variables, 23,232 binary variables, 654,720 equality constraints, and 1,059,168 inequality constraints. This level of complexity, as well as privacy protection and the uncertain scenarios, are the motivation for proposing the SP-ADMM approach. The simulation is conducted through a hybrid platform: MATLAB and GAMS. The hardware environment is a laptop with 1.90GHz CPU and 16.00GB RAM. The utility-level sub-problem is solved by MINOS, and the house-level sub-problems are solved by SCIP.

A. Parameter settings

The time resolution of the case study is 15 minutes, and the total time horizon is 24 hours. The total number of houses is 121. The number of residential houses allocated to different LAs are based on the original load at each bus in the IEEE 33-bus system [31].

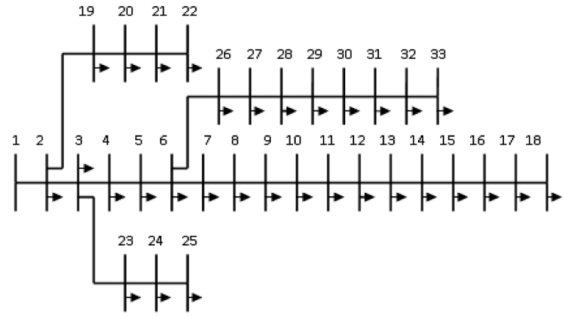

Fig. 3. Configuration of the IEEE 33-bus test system.

There are 31 houses that have HVAC systems, EWHs, and PVs installed, while the other 90 houses only have HVAC systems and EWHs installed. The discomfort weight factor for indoor temperature is \$0.05/°C, and the discomfort weight factor for water temperature is \$0.01/°C. The peak load violation rate is \$10/kW.

The outdoor temperature and standard solar output forecast information data for generating the test scenarios are plotted in Fig. 4, and the non-responsive load data for generating the test scenarios is shown in Fig. 5. Moreover, Monte Carlo sampling is employed to provide variation and uncertainty in different scenarios. The ranges of the uncertain parameters are given in TABLE I. Consequently, 100 samples are generated according to the probability distribution function of the uncertain parameters.

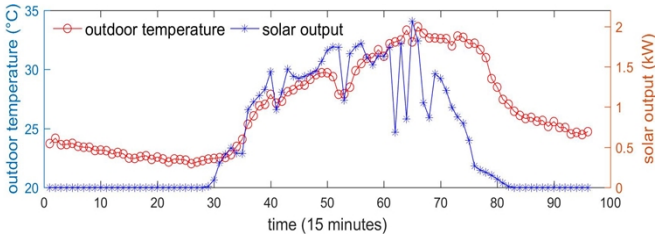

Fig. 4. Outdoor temperature and solar generation data for generating samples.

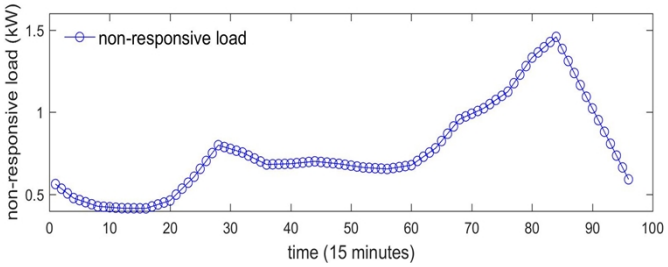

Fig. 5. Non-responsive load data for generating samples.

TABLE I. Range of Uncertain Parameters.

Parameter	Lower range	Upper range
Outdoor temperature	-20%	+20%
Solar output	-20%	+20%
Non-responsive load	-20%	+20%
Water consumption	-20%	+20%

Since it is computationally intensive to include all the samples into our considerations, a scenario reduction technique is conducted to reduce the computational burden [32]. The crux of this technique is to exploit a certain probability distance of the original and the reduced probability measure, and combine those scenarios that are close or have low probabilities [33]. Details on scenario reduction are available in [34]-[35]. In this work, the min-max normalization is first applied to preprocess different uncertain parameters [36]. Then the SCENRED tool in GAMS is employed as a black box to reduce the number of scenarios. The inputs to the SCENRED tool are the original

uncertain scenarios and their associated probabilities. The outputs from the SCENRED tool are the reduced uncertain scenarios and their new probabilities. Finally, the initial 100 samples are decreased to 10 scenarios considering the tradeoff between accuracy and computational time. The resulting probabilities of the reduced scenarios are given in TABLE II. Note, according to [37]-[38], there is no guarantee that increasing the number of scenarios will yield better results, since after passing a certain "sweet point", selecting more scenarios does not necessarily bring performance improvement on modeling the scenario distribution (i.e., performance improvement is saturated). The impact of scenario reduction on system performance will be further discussed in Section V.C.1 of this paper.

TABLE II. PROBABILITY OF EACH SCENARIO.

Scenario	1	2	3	4	5	6	7	8	9	10
Probability	0.08	0.11	0.04	0.16	0.11	0.07	0.13	0.16	0.07	0.07

TABLE III. PEAK LOAD IN DIFFERENT CASES.

Scenarios	1	2	3	4	5	6	7	8	9	10	avg.
Case1 (kW)	407.18	389.67	430.41	431.84	386.58	419.25	440.00	418.93	399.05	445.50	416.97
Case2 (kW)	405.17	421.09	394.31	387.78	413.54	407.80	376.09	407.27	413.44	396.79	401.36
Case3 (kW)	372.21	377.47	388.76	379.12	382.96	354.19	387.08	365.33	371.44	385.28	376.17

TABLE IV. PEAK LOAD VIOLATION IN DIFFERENT CASES.

Scenarios	1	2	3	4	5	6	7	8	9	10	avg.
Case1 (kW)	17.18	0	40.41	41.84	0	29.25	50.00	28.93	9.05	55.50	27.38
Case2 (kW)	15.17	31.09	4.31	0	23.54	17.80	0	17.27	23.44	6.79	13.52
Case3 (kW)	0	0	0	0	0	0	0	0	0	0	0

TABLE V. AVERAGE DISCOMFORT COST IN DIFFERENT CASES.

Scenarios	1	2	3	4	5	6	7	8	9	10	avg.
Case1 ($)	5.73	5.66	5.72	5.66	5.71	5.63	5.61	5.61	5.68	5.64	5.66
Case2 ($)	3.90	3.78	3.87	3.69	3.80	3.72	3.59	3.57	3.66	3.74	3.71
Case3 ($)	3.72	3.63	3.70	3.53	3.65	3.57	3.46	3.44	3.51	3.57	3.56

TABLE VI. AVERAGE ELECTRICITY COST IN DIFFERENT CASES.

Scenarios	1	2	3	4	5	6	7	8	9	10	avg.
Case1 ($)	5.93	4.50	7.84	8.01	4.56	6.85	8.64	6.86	5.27	9.16	6.78
Case2 ($)	5.67	6.99	4.77	4.23	6.37	5.92	4.45	5.82	6.41	4.98	5.51
Case3 ($)	4.29	4.29	4.29	4.29	4.33	4.25	4.33	4.32	4.38	4.40	4.32

Three test cases are designed to compare the performance of different DR management approaches. In Case 1, the responsive devices do not change their operating status unless the indoor/water temperature falls out of the pre-specified boundaries (i.e., conventional basic rule-based thermostat control). In Case 2, the DSO treats uncertain parameters as fixed values and applies the deterministic ADMM to coordinate the operating schedule of responsive devices. Finally, Case 3 implements the SP-ADMM to manage the operating schedules of residential components.

B. Simulation results

TABLE III compares the resulting load profiles in different cases. In Case 1, the peak load of the DSO is 445.50 kW and appears in Scenario 10 after the scenario reduction. The weighted average peak load of the DSO for all the scenarios is 416.97 kW. Therefore, both the peak and average loads exceed the 390-kW contracted load limit. In Case 2, the peak load of the DSO is 421.09 kW and appears in Scenario 2 after the scenario reduction. The weighted average peak load of the DSO for all the scenarios is 401.36 kW. In Case 3, the peak load of the DSO is further reduced to 388.76 kW, and it appears in Scenario 3 after the scenario reduction. The weighted average peak load of the DSO for all the scenarios is 376.17 kW.

TABLE IV provides the peak load violation in different cases. It is observed that the highest peak load violation appears in Case 1, which is 27.38 kW. By applying the deterministic ADMM approach, the peak load violation is decreased to 13.52 kW. The proposed SP-ADMM algorithm can further reduce the peak load charge to 0 kW. From Fig. 6 and the tables, it can be concluded that the SP-ADMM approach can significantly reduce the peak load and peak demand violation charge as compared to the conventional and deterministic ADMM controls. Under the SP-ADMM control mode, the DSO can coordinate the operating schedules of responsive devices through pre-cooling/pre-heating and avoid the situation where responsive devices are switched on at the same time, leading to performance improvement. The impacts of uncertainties are also considered, which further contributes to improved performance.

TABLE V and TABLE VI provide the average discomfort cost and electricity cost of each house in different scenarios. It is observed that the customers in Case 1 are expected to have more discomfort and pay higher costs than the customers in the other two cases. The sum of discomfort and electricity cost in Case 1 is $12.43. In Case 2, either the discomfort or electricity cost is lower than that in Case 1. The total cost is reduced to $9.22, which is only about 74.18% of the cost in Case 1. In Case 3, the sum of the discomfort and electricity cost is $7.87, which is 63.31% of the cost in Case 1. Therefore, Case 3 gives the best performance.

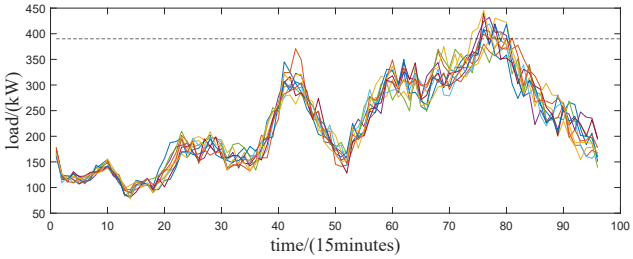

(a) Case 1

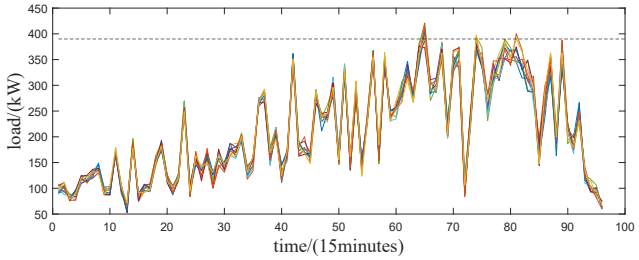

(b) Case 2

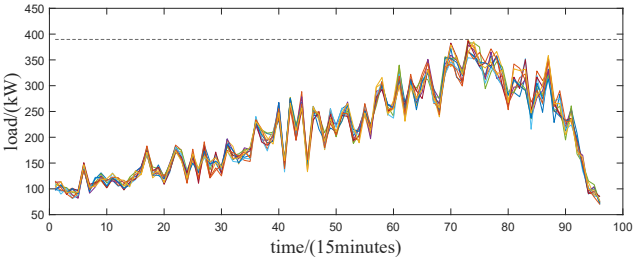

(c) Case 3

Fig. 6. Load profiles in different cases.

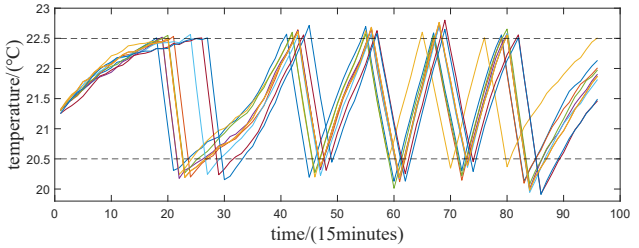

(a) Case 1

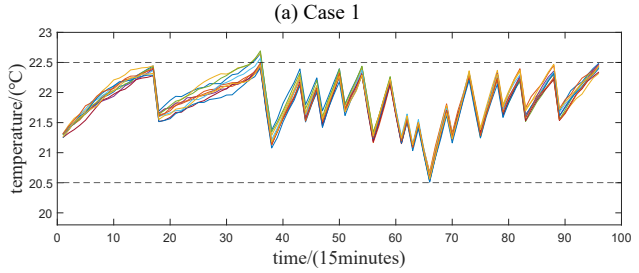

(b) Case 2

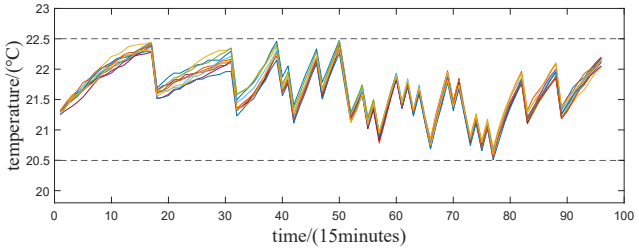

(c) Case 3

Fig. 7. Indoor temperature of house 1 in different cases.

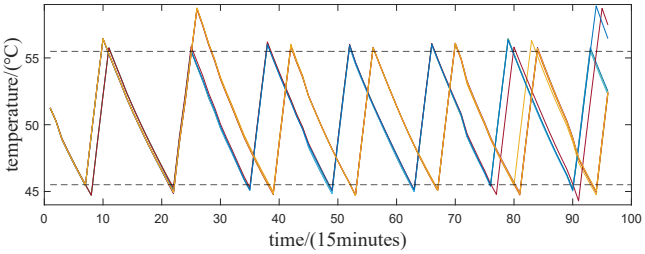

(a) Case 1

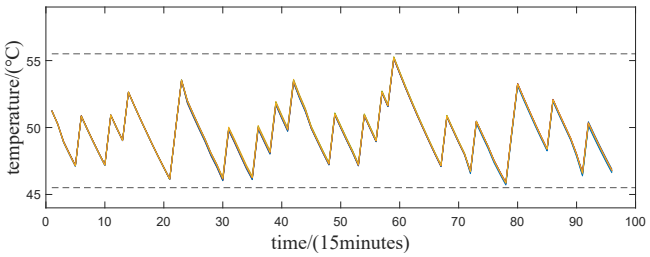

(b) Case 2

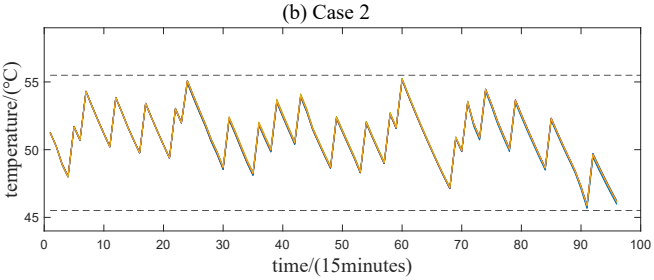

(c) Case 3

Fig. 8. Water temperature of house 1 in different cases.

Fig. 7 shows the impact of uncertainties on indoor temperature. The minimum and maximum indoor temperature limits for house 1 are 20.50℃ and 22.50℃, respectively. In Case 1, the indoor temperature range of house 1 in all the scenarios is from 19.91℃ to 22.80℃. In Case 2, the indoor temperature range of house 1 in all the scenarios is from 20.51℃ to 22.69℃. In Case 3, the indoor temperature range of house 1 in all the scenarios is from 20.51℃ to 22.47℃. From Fig. 7, it is observed that the indoor temperature deviation in Case 1 is much larger than that in the other two cases. Furthermore, due to the outdoor temperature uncertainty, the indoor temperature in Case 2 may violate the temperature constraints. In contrast, the indoor temperature in Case 3 is always within the pre-defined limits.

Fig. 8 shows the water temperature of house 1 in different cases. The minimum and maximum water temperature limits for house 1 are 45.50℃ to 55.50℃, respectively. In Case 1, the water temperature range of house 1 in all the scenarios is from 44.30℃ to 58.90℃. In Case 2, the water temperature range of house 1 in all the scenarios is from 45.71℃ to 55.28℃. In Case 3, the water temperature range of house 1 in all the scenarios is from 45.66℃ to 55.27℃. Therefore, the water temperature in Case 2 and Case 3 satisfy the pre-defined limits.

C. Discussions

1) Impact of scenario reduction

This sub-section studies the impact of scenario reduction on optimization results. First, three test cases are created, with each case having a different number of scenarios. Then the optimal HVAC and EWH operating schedules for these cases are solved and substituted back to the original 100 samples to evaluate the system performance. The results are given in TABLE VII. The table shows that the average peak load in all three cases falls below the 390-kW contracted limit, and the average load violations in the three cases are 5.09 kW, 5.18 kW, and 5.16 kW, respectively. Moreover, when the number of scenarios is 10, residential customers would pay less money for electricity but are also expected to have more discomfort than other cases. From the results, it is concluded that the difference among the results in the three cases is not significant, and therefore setting

the number of scenarios to 10 does not much affect the system performance.

TABLE VII. IMPACT OF SCENARIO REDUCTION ON RESULTS.

No. of scenarios	10	15	20
Avg. peak load (kW)	388.05	380.93	384.63
Avg. load violation (kW)	3.22	0.36	1.08
Avg. discomfort cost ($)	4.45	4.17	4.21
Avg. electricity cost ($)	5.09	5.18	5.16

2) Energy imbalance between day-ahead purchase and actual load in different scenarios

TABLE VIII shows the energy imbalance between the day-ahead purchase and actual load in different scenarios due to the weather and customer behavior uncertainties. From the table, it is observed that the weighted average daily energy surplus is 96.03 kWh, and the weighted average daily energy deficiency is 148.53 kWh. Therefore, only 4.78% of the electricity is cleared in the real-time market, and the effectiveness of the proposed method is justified.

TABLE VIII. ENERGY IMBALANCE BETWEEN DAY-AHEAD PURCHASE AND ACTUAL LOAD.

Scenario	1	2	3	4	5	6
Surplus (kWh)	76.22	92.95	103.09	109.72	92.95	103.67
Deficiency (kWh)	146.37	145.97	133.65	130.20	135.96	133.45
Scenario	7	8	9	10	avg.	
Surplus (kWh)	93.72	103.17	100.98	86.38	96.03	
Deficiency (kWh)	150.43	159.44	180.54	179.77	148.53	

3) Worst-case scenario

TABLE IX presents the worst-case scenarios under the conventional control (i.e. basic rule-based thermostat control), deterministic ADMM control, and SP-ADMM control, respectively. First, the optimal operating schedules in the three different approaches are solved and then substituted back to the original 100 samples to identify the worst-case scenario. In this work, the worst-case scenario is defined as the scenario with the largest objective function value. As shown in the table, the worst-case scenarios are different under the three control modes, and the SP-ADMM approach has the best performance in all categories since it has the least electricity cost, discomfort cost, and load violation.

TABLE IX. WORST CASE SCENARIO UNDER DIFFERENT CONTROL MODES.

	Conventional	Deterministic	SP-ADMM
Worst scenario number	48th	21st	38th
Avg. electricity cost ($)	9.52	7.61	5.64
Avg. discomfort cost ($)	5.66	3.83	3.68
Load violation (kW)	61.98	38.39	16.57

In addition, TABLE X compares average costs and load violations of the different approaches in the worst-case scenario for the SP-ADMM approach (i.e., scenario no. 38). Still, the SP-ADMM approach has the best performance of the three. However, it is observed from the table that the peak load in the SP-ADMM approach exceeds the desired maximum load limit in the worst-case scenario. This is reasonable because the SP-ADMM approach does not intend to guarantee the performance for the worst case, and the load violation is a soft constraint and is added to the objective function as a penalty term (i.e., occasional small violations can be tolerated). If the load violation is a hard constraint indeed, other models like robust optimization or hard constraints should be applied. This may be an area of research for future works.

TABLE X. COMPARISON OF DIFFERENT APPROACHES IN THE WORST-CASE SCENARIO FOR SP-ADMM.

	Conventional	Deterministic	SP-ADMM
Scenario number	38th	38th	38th
Avg. electricity cost ($)	8.34	5.92	5.64
Avg. discomfort cost ($)	5.69	3.84	3.68
Load violation (kW)	45.36	17.95	16.57

4) Switching frequency of the responsive devices

Another observation from the case study is that the switching frequency of the responsive devices in the conventional control mode is less than that in the SP-ADMM control mode (e.g., 11 times/day versus 35 times/day in house 1). The reason is that under the conventional control mode, the responsive devices are not allowed to change their operating status until the temperature falls out of the set bounds. However, this limit does not hold in the SP-ADMM control mode. Since frequently switching on/off the devices may reduce the lifespan of HVAC systems and EWHs, the time interval is set to 15 minutes in this work, which is sufficiently long to avoid the short-cycling problem [39].

5) Computational time

The computational time of the proposed SP-ADMM approach is given in TABLE XI. The proposed approach takes eleven iterations to converge. Since the house-level optimization is run in parallel, the computational time of each iteration is determined by the house that has the largest computational time. Also, the house-level model is a mixed-integer quadratic programming problem, and the first iteration has the longest computational time (for initializing the problem). For the utility-level, it only takes around 1.5 seconds to finish the calculation in each iteration. The total computational time for solving the residential DR problem with the SP-ADMM approach is 6 minutes and 32 seconds. As the communication delay among different agents is not considered in this paper, the time consumption in practical applications should be slightly longer than the times in TABLE XI. From the table, it is concluded that the proposed algorithm satisfies the computational time requirements for residential DR applications.

TABLE XI. COMPUTATIONAL TIME OF THE PROPOSED ALGORITHM.

Iteration	1	2	3	4	5	6
DSO (*sec*)	1.39	1.16	1.23	0.99	1.50	1.38
House (*sec*)	305.91	11.90	4.43	24.09	4.23	11.82
Iteration	7	8	9	10	11	
DSO (*sec*)	1.45	1.43	1.47	1.37	1.40	
House (*sec*)	3.25	3.30	3.17	2.91	2.69	

VI. CONCLUSIONS

This paper presents a comprehensive scheduling framework for scalable residential DR programs considering day-ahead and real-time electricity market operations. Due to the computational complexity and privacy concerns, the model is not suitable to be solved by the DSO as a centralized optimization, especially when multiple uncertain scenarios must be considered in the DR programs. Therefore, this paper proposes a new algorithm combining stochastic programing and the ADMM to form the SP-ADMM approach, which can decompose the original centralized DR scheduling model to a utility-level problem and house-level sub-problems to distribute the computational complexity and to incorporate multiple uncertain scenarios.

The case study demonstrates that the proposed approach can reduce customers' electricity bills, discomfort, and the peak load at the utility level. Also, since the optimization model is

solved in a distributed manner, increasing the number of houses will not affect the number of variables in each sub-problem. Hence, it will not significantly impact the computing performance in large scale applications. The information exchange among the utility, LAs, and consumers is limited to the real and reactive power consumption and the primary residuals and dual variables in each scenario, which protects the customers' privacy. Finally, the results show that the proposed SP-ADMM model can improve residential DR performance and reduce the chance of constraint violations as compared to the conventional and deterministic ADMM approaches.

In this work, the voltage magnitudes are always within the typically allowable range of [0.95, 1.05]. Therefore, the voltage magnitude constraints are not included in the problem formulation. However, distribution networks may suffer from low-voltage problems at the end of feeders in practical applications, especially when the system is heavily loaded, or the uncertainty is large. If the DSO has high requirements for maintaining the voltage levels, more conservative demand management approaches should be applied. We would like to address this problem in our future works.

APPENDIX: MODELING OF THERMOSTAT-CONTROLLED LOADS

A simplified version of the resistance-capacitance (RC) thermal model is applied to capture the temperature dynamics of thermostat-controlled loads in this work. The RC model is constituted with an electrical analog pattern with resistance (R) and capacitance (C), which are obtained from historical data by using linear regressions. It has a "visible" model structure and therefore can be used for optimal controls of responsive devices.

For HVAC systems, the input parameters are the day-ahead forecasted outdoor temperature in different scenarios. The HVAC model is represented by (26), and its discrete-time version is represented by (6). Similarly, the discrete-time version of the EWH model is described in (9).

- $C_i^{house}\frac{dT_{i,t}^{in}}{dt} = (T_t^{out} - T_{i,t-1}^{in})/R_i^{house} - b_{i,t}^{hvac} \cdot p_i^{hvac}$ (26)

The parameter settings of the HVAC system are given in TABLE XII, and the power factor of the HVAC is set to 0.81. The parameter settings of the EWH are given in TABLE XIII, and the power factor of the EWH is set to 1.

TABLE XII. HVAC PARAMETER SETTINGS.

Chouse i	*U*[1.0, 1.5] J/℃	*Rhouse i*	*U*[6.4, 9.6] J/℃
Phvac i	3.5 kW	*Tins i*	*U*[21, 23] ℃
$\underline{T}$*in i*	*Tins i*-1℃	$\bar{T}$*in i*	*Tins i*+1℃

TABLE XIII. EWH PARAMETER SETTINGS.

Cwh i	*U*[0.1, 0.15] J/℃	*Rwh i*	*U*[48.0, 72.0] J/℃
Pwh i	2.5 kW	*Twhs i*	*U*[55.0, 57.5] ℃
$\underline{T}$*wh i*	*Twhs i*-5℃	$\bar{T}$*wh i*	*Twhs i*+5℃

Acknowledgment

Research sponsored by the Laboratory Directed Research and Development Program of Oak Ridge National Laboratory, managed by UT-Battelle, LLC, for the U.S. Department of Energy.

REFERENCES

[1] F. Chen, F. Li, W. Feng, et al., "Reliability assessment method of composite power system with wind farms and its application in capacity credit evaluation of wind farms," *Electric Power Systems Research*, vol. 66, pp. 73-82, Jan. 2019.

[2] Y. Du, and F. Li, "A Hierarchical Real-time Balancing Market Considering Multi-microgrids with Distributed Sustainable Resources," *IEEE Transactions on Sustainable Energy*, vol. 11, no. 1, pp. 72-83, Jan. 2020.

[3] M. Starke and N. Alkadi, "Assessment of industrial load for demand response across US regions of the western interconnect," Oak Ridge National Laboratory, ORNL/TM-2013/407, 2013.

[4] U.S. Environmental Protection Agency, "About the U.S. electricity system and its impact on the environment," [Online] Available: https://www.epa.gov/energy/about-us-electricity-system-and-its-impact-environment.

[5] X. Kou, F. Li, J. Dong, et al., "A distributed energy management approach for residential demand response,", *3rd International Conference on Smart Grid and Smart Cities*, pp. 1-6, Berkeley, CA, June 2019.

[6] H. Zandi, E. Vineyard, J. Sanyal, et al., "Home energy management retrofit control platform," *12th IEA Heat Pump Conference*, pp. 1-10, May 2017

[7] P. Yi, X. Dong, A. Iwayemi, et al., "Real-time opportunistic scheduling for residential demand response," *IEEE Transactions on Smart Grid*, vol. 4, no. 1, pp. 227-234, Mar. 2013.

[8] M. Pedrasa, T. Spooner, and I. MacGill, "Coordinated scheduling of residential distributed energy resources to optimize smart home energy services," *IEEE Transactions on Smart Grid*, vol. 1, no. 2, pp. 134-143, Sep. 2010.

[9] S. Pal and R. Kumar, "Electric vehicle scheduling strategy in residential demand response programs with neighbor connection," *IEEE Transactions on Industrial Informatics*, vol. 14, no. 3, pp. 980-988, Mar. 2018.

[10] W. Zheng, W. Wu, B. Zhang, et al., "Distributed optimal residential demand response considering operational constraints of unbalanced distribution networks," *IET Generation, Transmission & Distribution*, vol. 12, no. 9, pp. 1970-1979, May 2018.

[11] K. Worthmann, C. Kellett, P. Braun, et al., "Distributed and decentralized control of residential energy systems incorporating battery storage," *IEEE Transactions on Smart Grid*, vol. 6, no. 4, pp. 1914-1923, July 2015.

[12] X. Kou, and F. Li, "Interval optimization for available transfer capability (ATC) evaluation considering wind power uncertainty," *IEEE Transactions on Sustainable Energy*, vol. 11, no. 1, pp. 250-259, Dec. 2018.

[13] M. Diekerhof, F. Peterssen, and A. Monti, "Hierarchical Distributed Robust Optimization for Demand Response Services," *IEEE Transactions on Smart Grid*, vol. 9, no. 6, pp. 6018-6029, Nov. 2018.

[14] M. Shafie-Khah, and P. Siano, "A stochastic home energy management system considering satisfaction cost and response fatigue," *IEEE Transactions on Industrial Informatics*, vol. 14, no. 2, pp. 620-6029, Nov. 2018.

[15] Z. Chen, L. Wu, and Y. Fu, "Real-time price-based demand response management for residential appliances via stochastic optimization and robust optimization," *IEEE Transactions on Smart Grid*, vol. 3, no. 4, pp. 1822-1831, Dec. 2012.

[16] M. Almassalkhi, L. Espinosa, P. Hines, et al., "Asynchronous coordination of distributed energy resources with packetized energy management," Energy Markets and Responsive Grids, Springer, New York, NY, 2018, pp. 333-361.

[17] J. Mathieu, M. Kamgarpour, J. Lygeros, et al., "Arbitraging intraday wholesale energy market prices with aggregations of thermostatic loads," *IEEE Transactions on Power Systems*, vol. 30, no. 2, pp. 763-772, Mar. 2015.

[18] J. Mathieu, S. Koch, and D. Callaway, "State estimation and control of electric loads to manage real-time energy imbalance." *IEEE Transactions on Power Systems*, vol. 28, no. 1, pp. 430-440, Feb. 2013.

[19] A. Safdarian, M. Fotuhi-Firuzabad, and M. Lehtonen, "A distributed algorithm for managing residential demand response in smart grids," *IEEE Transactions on Industrial Informatics*, vol. 10, no. 4, pp. 2385-2393, Nov. 2014.

[20] M. Bozchalui, S. Hashimi, H. Hassen, et al., "Optimal operation of residential energy hubs in smart grids," *IEEE Transactions on Smart Grid*, vol. 3, no. 4, pp. 1755-1766, Dec. 2012.
[21] O. Alrumayh, and K. Bhattacharya, "Flexibility of residential loads for demand response provisions in smart grids," *IEEE Transactions on Smart Grid*, vol. 10, no. 6, pp. 6284-6297, Nov. 2019.
[22] X. Kou, F. Li, J. Dong, et al., "A scalable and distributed algorithm for managing residential demand response programs using alternating direction method of multipliers (ADMM)," *IEEE Transactions on Smart Grid*, in-press.
[23] A. Levitt, "Comparing RTO market framework Rules in DER context," [Online] Available: http://www.pjm.com/~/media/committees-groups/committees/mrc/20160824-special/20160824-item-02-der-rto-benchmarking.ashx.
[24] R. Henriquez, G. Wenzel, D. Olivares, et al., "Participation of demand response aggregators in electricity markets: Optimal portfolio management," *IEEE Transactions on Smart Grid*, vol. 9, no. 5, pp. 4861-4871, Feb. 2017.
[25] K. Ponds, A. Arefi, A. Sayigh, et al., "Aggregator of demand response for renewable integration and customer engagement: strengths, weaknesses, opportunities, and threats," *Energies*, vol. 10, no. 9, pp. 2391-2410, Sep. 2018.
[26] B. Bhattarai, K. Myers, B. Bak-Jensen, et al., "Optimum aggregation of geographically distributed flexible resources in strategic smart-grid/microgrid locations," *International Journal of Electrical Power & Energy Systems*, vol. 92, pp. 193-201, Nov. 2017.
[27] C. Li, X. Yu, W. Yu, et al., "Efficient computation for sparse load shifting in demand response management," *IEEE Transactions on Smart Grid*, vol. 8, no. 1, pp. 250-261, Jan. 2017.
[28] EPCOR, "Terms and conditions for distribution connection services," Alberta, Canada, 2016.
[29] L. Gan and S. Low, "An online gradient algorithm for optimal power flow on radial networks," *IEEE Journal on Selected Areas in Communication*, vol. 34, no. 3, pp. 625-638, Mar. 2016.
[30] S. Boyd, N. Parikh, E. Chu, et al., "Distribution optimization and statistical learning via the alternating direction method of multipliers," *Foundations and Trends in Machine Learning*, vol. 3, no. 1, DOI: 10.1561/220000000016, 2010.
[31] M. Baran, and F. Wu, "Network reconfiguration in distribution systems for loss reduction and load balancing," *IEEE Transactions on Power Delivery*, vol. 11, no. 4, pp. 1401-1407, Apr. 1989.
[32] Y. Chen, and M. Hu, "Swarm intelligence-based distributed stochastic model predictive control for transactive operation of network building clusters," *Energy and Buildings*, vol. 198, no. 1, pp. 207-215, Sep. 2019.
[33] GAMS Development Corporation, General Algebraic Modeling System (GAMS) Release 27.1.0, Fairfax, VA, USA, 2019.
[34] J. Dupacova, N. Growe-Kuska, and W. Romisch, "Scenario reduction in stochastic programming: An approach using probability metrics," *Mathematical Programming*, vol. 95, pp. 493-511, Mar. 2003.
[35] H. Heitsch, and W. Romisch, "Scenario reduction algorithms in stochastic programming," *Computational Optimization and Applications*, vol. 24, pp. 187-206, Feb. 2003.
[36] S. Raschka, "Data preprocessing and machine learning with Scikit-Learn," [Online] Available: https://sebastianraschka.com/pdf/lecture-notes/stat479fs18/05_sklearn_slides.pdf.
[37] Y. Wang, "Energy storage operation with wind uncertainty," Ph.D. dissertation, University of Washington, Seattle, WA, 2017.
[38] Y. Wang, Z. Zhou, C. Liu, et al, "System evaluation of stochastic methods in power system scheduling and dispatch with renewable energy," Argonne National Laboratory, ANL/ESD-16-10, Aug. 2016.
[39] B. Sanandaji, T. Vincent, and K. Poolla, "Ramping rate flexibility of residential HVAC loads," *IEEE Transactions on Sustainable Energy*, vol. 7, no. 2, pp. 865-874, Apr. 2016.
[40] B. Cui, F. Chen, J. Munk, et al., "A hybrid building thermal modeling approach for predicting temperatures in typical, detached, two-story houses," *Applied Energy*, vol. 236, pp. 101-116, Feb. 2019.